JOURNAL OF THERMOPHYSICS AND HEAT TRANSFER
Vol. 6, No. 3, July–Sept. 1992

Effect of Surface Material Properties and Surface Characteristics in Evaporative Spray Cooling

M. S. Sehmbey,* M. R. Pais,† and L. C. Chow‡
University of Kentucky, Lexington, Kentucky 40506

In the spray cooling of a heated surface, variations in the surface contact angle cause a change in nucleation characteristics and, thereby, influence the heat transfer process; a higher contact angle shows an enhanced heat transfer due to the ease in nucleation caused by the lowered free energy associated with bubble formation. Results are presented for different surface coatings and spray configurations. The surface roughness variation influences the flowfield, altering the maximum liquid film thickness, the bubble diameter, vapor entrapment, bubble departure characteristics, and, thereby, the ability of the surface to transfer heat. The effect of surface roughness on spray cooling is also studied.

Nomenclature

A = surface area
D = apparent diameter of a drop
d = diameter of a drop
F = free energy
f = surface profile function
K = thermal conductivity
p = pressure
q = heat flux
r = radius
T = temperature
Γ = latent heat of vaporization
θ = contact angle
λ = roughness spacing
v = specific volume
σ = surface tension
ϕ = angle of contact on vapor side

Subscripts
Cu = copper
Co = constantan
lg = liquid/gas interface
m = minimum
s = saturation
w = wall

Superscript
$''$ = vapor phase

Introduction

CURRENT heat transfer enhancement research has been directed toward phase change processes. Such processes take advantage of the fact that a pure substance will absorb or release heat at a fixed temperature. The exchange of this latent heat is feasible at low degrees of superheat, and, depending on the surface, the magnitude can be far greater than the corresponding sensible heat exchange for the same temperature difference.

Spray cooling[1–3] in particular has proved to be far more efficient than the conventional pool-boiling method of heat removal.[4–7] This is partially because the hydrodynamic instabilities inherent in pool boiling in the region of the critical heat flux (CHF) are precluded by the deposition of a thin film of liquid[8,9] on the surface in spray cooling. The objective of this work is to study the effect of the surface material contact angle and the surface roughness on heat transfer phenomena involved in spray cooling.

The phenomenon of wettability plays an important part in nucleation and boiling.[10–13] The effect of contact angle is most pronounced at CHF in pool boiling, a lower contact angle provides better wetting and, thus, a higher transition heat flux.[11–13] The effect of contact angle on spray cooling has not been studied earlier and this is one of the purposes of this study.

Referring to Fig. 1, the free energy of formation ΔF of a vapor nucleus of radius r_{lg}, for a contact angle $\theta = \pi - \phi$, and surface tension σ_{lg}, can be written as[14]

$$\Delta F = \tfrac{2}{3}\,\sigma_{lg}\pi r_{lg}^2(1 - \cos\phi - \tfrac{1}{2}\cos\phi\sin^2\phi) \qquad (1)$$

Hence, for $\phi \to 0$ the value of the free energy change $\Delta F \to 0$, and for $\phi = \pi$, $\Delta F = \Delta F_{\text{sphere}}$. A deduction of the above analysis indicates that, because

$$\phi = \pi - \theta \qquad (2)$$

the contact angle must be π (i.e., $\phi = 0$) for maximizing vapor nucleus generation. However, this would create a vapor film on the surface that would drastically reduce the heat transfer. Also, the liquid would not spread on the surface, thus creating hot spot regions leading to dryout. If the contact angle $\theta \to 0$; i.e., the liquid wets the surface completely, then $\phi \to \pi$; this demands the maximum change in free energy for nucleation. In wetting the whole surface, the liquid provides maximum contact between the coolant and the heat dissipat-

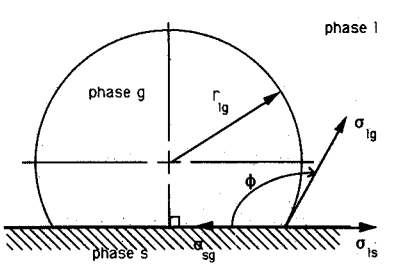

Fig. 1 Critical nucleus at liquid/solid.

Presented as Paper 90-1729 at the AIAA 5th Joint Thermophysics and Heat Transfer Conference, Seattle, WA, June 18–20, 1990; received July 26, 1990; revision received June 25, 1991; accepted for publication June 26, 1991.

*Graduate Research Assistant, Department of Mechanical Engineering. Member AIAA.
†Postdoctoral Research Associate, Department of Mechanical Engineering. Member AIAA.
‡Professor, Department of Mechanical Engineering. Member AIAA.

ing surface, but at the same time, suppresses nucleation. If evaporation from the free surface of the liquid is the dominating heat transfer mechanism, then the suppression of nucleation will be advantageous, because no resistance to heat transfer will arise due to the formation of a vapor barrier between the liquid and the hot surface. However, if the conduction resistance from the hot surface through the liquid to the free surface is large, then the nucleation phenomenon will play the controlling role. In such a case, a perfectly wetting liquid provides maximum liquid/solid contact but is not conducive to nucleation. On the other hand, a nonwetting liquid, although optimum for nucleation, does not provide sufficient liquid/solid contact, thus leading to dryout. For rough surfaces, entrapment of gas/vapor within the cavity is determined by $\theta >$ included angle formed by the cavity walls.[15] All this implies that a perfectly wetting liquid is not advantageous for the nucleation process, although it may be better near the dryout region.

By selecting different liquid/solid combinations variations in contact angle, θ can be obtained, and by spraying the liquid using a gas atomizing nozzle, the following can be achieved:

1) The liquid is forcefully spread over the surface by the secondary stagnation flow of the gas as a flat film, although $\theta > 0$, maximizing liquid/solid contact for heat transfer.

2) The flat film with the reduced vapor pressure at the free surface (due to the secondary stagnation flowfield of the gas that clears away the vapor produced) provide optimum conditions for evaporation at the liquid/ambient interface.

Figure 2 illustrates the physics of evaporation/boiling taking place within a thin film of liquid deposited on a hot surface by droplet impingement assisted by an external gas stagnation flowfield. If the film is ultrathin (of the order of a few microns in the case of water), then the heat can be conducted through the liquid to the surface, where the liquid will evaporate directly into the ambient. An air/droplet impingement field on the surface due to an air atomizing nozzle is shown in Fig. 2. Upon impinging the surface, the air jet forms a stagnation point flowfield. The drops do not follow the air streamlines close to the surface due to their relatively higher inertia. These drops impinge on the hot surface to form flat disks, whose thickness is much lower than the diameter of the drop.[16] Simultaneously, the stagnation flowfield spreads the droplets/disks further, through shear forces, to form a thin film on the surface. The vapor emanating due to evaporation is swept away by the stagnation air flowfield. Hence, the effect of the stagnation flowfield enhances evaporation further, by clearing away the vapor, thereby, reducing the vapor pressure in the vicinity of the free liquid surface. Thus, the possibility of phase change at or below 100°C; i.e., with negative superheats, exists for water at 1-atm ambient pressure. Also enhanced is wettability, (i.e., liquid/solid contact) for liquid/solid combinations that do not have contact angles near zero.

Concurrently, if the superheat is sufficient, nucleation will occur at the liquid-solid interface, the radius above which the bubble will survive and grow being given by[14]

$$r''_m = \frac{2\sigma v'' T}{\Gamma(T_w - T_s)} \tag{3}$$

In the case of nucleate boiling, roughness plays a governing role in the enhancement of heat transfer. Rough surfaces have been shown to exhibit a lower superheat for boiling because of the increase in vapor entrapment by the large cavities of a rough surface, which then act as nucleation sites.[15,17] Furthermore, the heat transfer also improves due to the increase in surface area subtended by the roughness elements.

The heat transfer and the nucleation site density depends upon the distribution of the roughness elements, i.e., primarily on λ, the spacing between the roughness elements.[7,18,19] Consider nucleation on a rough wall. As the density of the nucleation sites increases, at first the heat flux will increase, as would be expected. However, as the nucleation sites get closer, the growth of the bubbles created by adjacent sites will cause the bubbles to combine and form a vapor barrier, leading to dryout.[20-22] Hence, there may exist a configuration that produces the maximum heat flux at the lowest superheat, the spacing in this configuration, being far more than that for a densely packed surface.[23]

In spray cooling, the thermal boundary layer is limited by the thickness of the liquid film. The bubble, on emerging from the cavity and growing above the liquid film, will be exposed to temperature gradients and the forces of the external flowfield (see Fig. 2). The bubble temperature being higher, will induce its walls to evaporate into the ambient. Second, the temperature gradients in the vicinity will make the bubble unstable.[24,25] Third, the external droplet/ambient flowfield also physically assists in the early departure/breakup of the bubble. Thus, the bubble breaks up much sooner than it would in pool boiling or even in most cases of flow boiling. Thus, the formation of the vapor blanket on the surface is delayed, permitting a higher heat flux to be sustained.

A surface profilometer was used to obtain the surface profiles of the different surfaces used in this study. In all, two surface roughnesses were studied. The first surface was polished with 14-μm grit emery paper and the second surface was lapped with 0.3-μm lapping compound. To study the effect of contact angle, the surface polished using the 14-μm grit emery paper was successively plated with an extremely thin layer of nickel and gold, respectively. Next the surface coordinates for all of these surfaces were obtained using a diamond tip profilometer with a resolution of 0.1 μ. Profilometer measurements of the plated surfaces (presented under "Results and Discussion") indicate that the roughness value does not change appreciably with the addition of the plating. Second, because the thermal conductivity of the nickel and gold is high and the thickness of the plating is small, its resistance to heat transfer is considered negligible.

Experiments were performed on the surfaces described above for 1) different coolant flow rates; 2) atomizing air flow rates, which allow variation in both droplet size and droplet velocity; and 3) coolant temperature or degree of subcooling. Thus, this study provides information on the influence of surface conditions under various regimes of spray-cooling heat transfer.

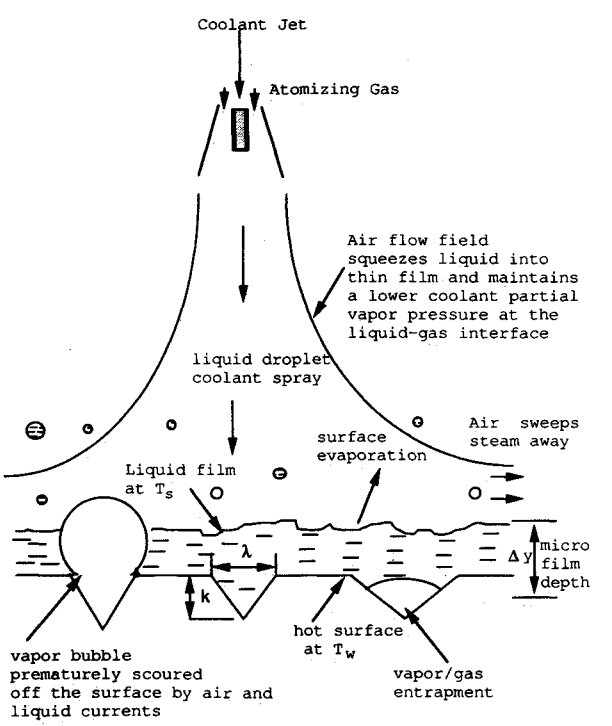

Fig. 2 Spray dynamics.

Surface Preparation

In all, three surface materials were tested. The first was an oxygen-free copper surface (the block material). The surface was polished in one direction only using 14-μm grit emery paper such that it had a definite "lay."[26] The second surface was prepared by electroplating the copper surface with nickel. The thickness of the coating being minimal, the temperature drop across it can be neglected, and it is assumed that the surface temperature is the same as that predicted for the bare copper surface. The third surface was similarly prepared by electroplating 24-carat gold over the nickel surface, again the thickness of gold coating was negligible (roughness values for the three surfaces are comparable, indicating similar roughness conditions; data are provided in "Results and Discussion"). For the surface roughness part of the experiments, two surfaces polished successively with 14-μm grit emery paper and 0.3-μm lapping compound, were tested.

Experimental Description

Because large thermal gradients are required to drive large heat fluxes through any surface (>1500 W/cm^2), care must be taken in the design of the apparatus in order to arrive at temperatures within the body that maintain the physical and chemical integrity of the system.

With reference to Fig. 3, high-power tungsten-in-quartz heat lamps are inserted into the lower cylindrical copper heater block of 33-mm diam × 25-mm high. This system; i.e., the tungsten filament, which can be viewed as a line element radiative heat source, (temperature = 2200°C, $0.5 \leq \lambda \leq 4.5$ μm), enclosed within a cylinder closed at its ends, constitutes a black body. Thus, all the radiative energy is absorbed into the copper block. This heat is then conducted through the pyramidal construction to the surface to be cooled. The design is such as to arrive at a uniform temperature on the surface to be cooled. These radiation lamps have a fast thermal response (99% rated power within 3 s), can withstand high temperatures by virtue of their sealed quartz envelope, and provide a high radiative heat flux. Depending on the heat flux required, a multiple number of these lamps can be used in this setup.

The temperature controller, shown in Fig. 3, monitors the temperature of the cooled surface, maintaining it at some preset value by sending a control signal to the phase-angle

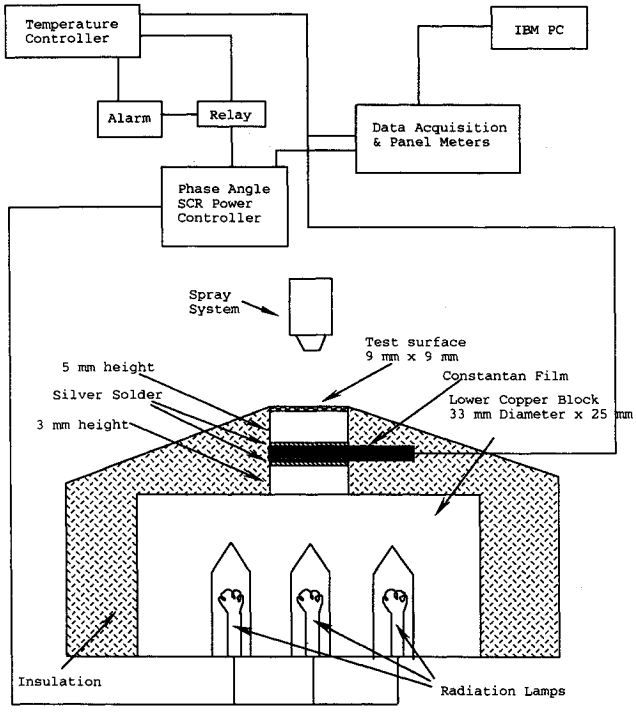

Fig. 3 Temperature measurement and control setup.

SCR power supply, which in turn regulates the power to the quartz lamps by varying the phase angle on each ac cycle proportional to the control signal. In the event of an overshoot in the temperature of the surface, an alarm disconnects the power to the heaters via relays. The power to the lamps along with the temperatures are continuously indicated by the panel meters and recorded by the data acquisition system. All process parameters are displayed and stored on the PC.

The heat source consists of two parts; namely, the lower cylindrical copper body with inserted radiation lamps; and the 9-mm × 9-mm-square crown (8 mm high) or cooled surface (shown in Fig. 3) from which heat removal is desired. The whole assembly (excluding the surface exposed to the spray) is insulated in high-temperature insulation to keep heat losses to a minimum. By measuring the temperature difference across a known distance in a section of the crown where the isotherms have flat profiles, the heat flux can be determined using Fourier's law of heat conduction.

At a desired heat flux of 1000 W/cm^2 in a copper body of uniform cross section, the temperature gradient is 25.4°C/mm. This requires that the size of the thermocouple be of the order of 40 μm for a temperature measurement resolution to be within 1°C. Temperature measurement using such fine thermocouples is not recommended at such high temperatures, being more susceptible to standard wire errors, corrosion, and failure. Second, an uncertainty analysis

$$\frac{w_q}{q} = \sqrt{\left[\frac{w_x}{\Delta x}\right]^2 + \left[\frac{w_T}{\Delta T}\right]^2} \tag{4}$$

implies that the prediction of the heat flux is also dependent upon accurate measurement of the distance between the two thermocouples Δx. Ideally, this is a parameter in the heat flux equation, which should be minimized for maximum temperature reduction within the system.

An alternative method of temperature measurement[27] would be to use a thin film of constantan (127 μm thick, in this case, selected because with copper it composes a thermocouple), interleaved between the copper surface on the top, (which constitutes the cooled surface shown in Fig. 3), and the heated copper block at the bottom, located in a region of the crown 3 mm above the lower copper block, where flat isotherms are predicted. Constantan has a low thermal conductivity, (21.12 W/mK), thus, the thinner the film, the lower the temperature rise across it. Second, the film thickness measurement Δx when accurately determined (127 ± 12 μm), further reduces the uncertainty in the heat flux prediction.

The thermocouple junction cannot be assumed to be isothermal because a heat flux exists across the solder layer (50–70 μm thick). Hence, a simple copper-constantan thermocouple calibration is invalidated. Therefore, copper-silver and silver-constantan calibrations were obtained and the corrected temperatures used in the calculation of the heat flux. Knowledge of the heat flux allows evaluation of surface temperature by extrapolation

$$T_{\text{surf}} = T_{\text{Co}} - q(\Delta x_{\text{Cu}}/K_{\text{Cu}}A) \tag{5}$$

Spray System

An air-atomizing nozzle was used to generate homogeneous droplet sprays over small areas (approximately 15-mm diameter). A thin (<0.5 mm) annular liquid stream of distilled, deionized water is aspirated or injected into the path of an accelerating jet of air (minimum jet diameter = 0.7 mm). Through surface shear forces, the air jet atomizes the liquid into small droplets (ranging in size from 7 to 25 μm, depending on liquid and air flow rates), and imparts momentum to them (6–61 m/s, see Table 1). The compressed air to drive the nozzle is supplied at 584 kPa with a relative humidity of nearly 100%. A regulating value is used to reduce the pressure of

the moist air; as a result, the exit relative humidity of air is found from calculations to be less than 30%.

Droplet Size and Velocity Measurement

Using a single-component phase-Doppler particle analyzer, droplet size and velocity distributions were obtained over the surface for a fixed set of air and water flow rates. Table 1 provides the flowfield parameters for ten different cases used in the experiments presented later.

Results and Discussion

Using the air-atomizing nozzle spray system, water was sprayed onto the surface at varying air and water flow rates. Table 1 provides the parameters of the flowfield for ten different cases of liquid and gas flow rates. A number of experiments were performed to check for repeatability, occurrence, and value of the critical heat flux (CHF). The experiments are repeatable in heat flux within ± 50 W/cm^2 and ± 2°C in surface temperature. At the lower coolant flow rates, the control of the flow was within ± 0.3 l/h. Experiments were begun at room temperature and ramped up continuously until Leidenfrost conditions were reached. The heaters were then switched off and the recorded data analyzed. The power was ramped up slowly enough to ensure that the measurements were quasisteady. Heating up and cooling cycles were performed up to and prior to the CHF region. The hysteresis noted was minimal, indicating a negligible effect of any existing transient conditions. The block was gradually heated to higher temperatures by increasing the set-point temperature of the controller. The surface temperature was, thus, increased to about 210°C in most cases; the dryout occurred in the range of 200–215°C for all the cases.

Figure 4 shows the effect of varying the water flow rate at a constant air flow rate for a copper surface polished with 14-μm emery paper. It can be seen that increasing the water flow increases the heat flux at any given temperature. At lower temperatures, the instantaneous local heat transfer coefficient in the region of droplet impact increases with the increasing flow rate, thereby arising in an increase in the overall heat transfer over the whole surface. It was seen that there occurred a saturation of heat flux, (i.e., there was no increase in heat transport for further temperature rise of the surface > 180°C) in the case of water flow rate of 1 l/h. This was due to the fact that, for this flow rate, almost all the water falling on the surface evaporates, thus, an increase in temperature beyond a certain point leads to little change in heat flux until the dryout temperature is reached.

Figure 5 shows the effect of varying the air flow rate on the heat flux for a copper surface polished with 14-μm emery paper. As the air flow rate is increased, for the same liquid flow rate of 1 l/h, a thinner liquid film is expected on the surface. This is true because, first, the droplets are smaller in diameter and have higher velocities, which upon impinging the surface will flatten to thinner disks. Second, the stagnation flowfield due to the air has increasing ability not only to squeeze the film thinner, but also to sweep away the evaporating vapor, creating a lower partial vapor pressure on the surface of the liquid. Below 100°C, subcooled liquid forced convection and evaporation play an important part. The droplets impact with higher velocities as the air flow rate increases (see Table 1). Hence, the instantaneous local heat transfer coefficient in the region of impact is higher, leading to an overall higher heat transfer rate as evidenced from Fig. 5.

Comparing the effect of air flow rate and water flow rate, it can be seen that air flow rate has a more pronounced effect

Table 1 Experimental flowfield parameters

Water flow rate, l/h	Drop size range, μm	Average velocity, m/s	Air pressure/ flow rate, psig, l/s
4.0	15–20	10–55	60/0.32
4.0	16–20	8–46	40/0.25
4.0	17–25	6–42	20/0.16
2.0	9–16	27–61	60/0.32
2.0	10–16	19–50	40/0.25
2.0	14–20	13–32	20/0.16
1.0	7–14	9–47	75/0.38
1.0	8–14	9–44	60/0.32
1.0	9–15	10–38	40/0.25
1.0	11–15	7–28	20/0.16

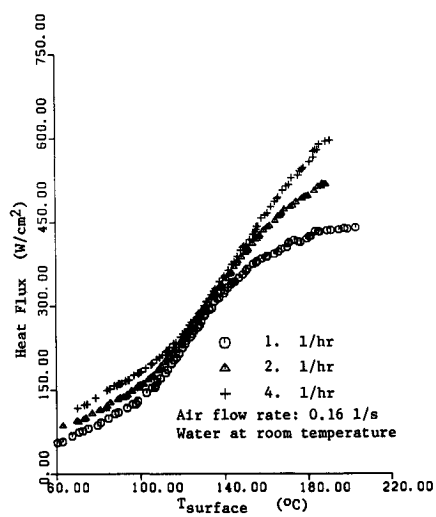

Fig. 4 Effect of water flow rate.

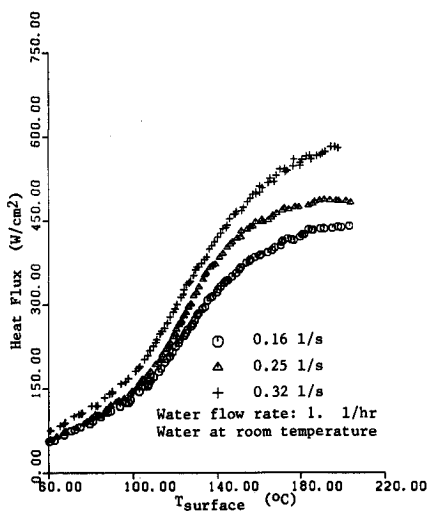

Fig. 5 Effect of air flow rate.

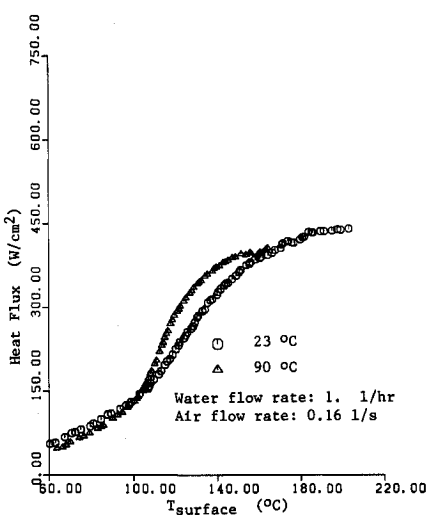

Fig. 6 Effect of subcooling.

in the temperature range of 100°C to about 160°C. An increase in water flow rate tends to have very little effect on the heat flux vs temperature curve in this temperature range because a higher water flow rate results in a thicker liquid film that decreases the evaporation from the free surface, thus canceling out the effect of increased convection. On the other hand, an increase in air flow rate leads to a thinner film, increased convection, and reduced partial vapor pressure. At higher temperatures (>160°C) the amount of water falling on the surface becomes more important because of increased phase change at these elevated temperatures.

The effect of coolant temperature at a flow rate of 1 l/h on a copper surface polished with 14-μm emery paper is shown in Fig. 6. As seen the heat flux for the higher temperature coolant is lower at first, this is because in the initial stages the heat transfer is mainly sensible heating of the coolant and this will be lower for the coolant at higher temperature. At around 100°C the slope of the curve for the hotter coolant changes dramatically as compared to the room temperature coolant. This is because the hotter coolant requires lesser sensible heating before phase change, hence, more of it vaporizes as compared to the cooler fluid. As the temperature of the surface increases the higher temperature coolant spray reaches the saturation heat flux (region of little slope before CHF) earlier than the cooler fluid spray. The saturation heat flux is lower as it lacks the sensible heating part (which makes up about 10–15% of the total heat flux) of the heat transfer process as compared to the cooler fluid spray.

Contact Angle Effects

As mentioned earlier (see "Surface Preparation") three different surface materials were used for studies concerning the effects of wettability on spray cooling. It is well known that gold has a very high contact angle (all contact angles are with reference to water) as compared to copper and nickel. In fact, nickel has almost the same contact angle as copper.[17] Contact angle measurements were done using a contact angle viewer that provides a magnification of ×40. In order to measure the contact angles of the surfaces used in the experiments a thin strip of copper (about 75-mm-long) was coated with nickel for one-third of its length, the next one-third was left bare, and the last section was coated with gold. The process used for the coatings was exactly the same as that used in the experiments. The surface was then cleaned with methanol and a drop of water was put on each of the three sections. The instrument was then used to view a magnified profile of the drop and measure the static contact angle by aligning a protractor tangential to the drop at the liquid/solid interface. Thus, all the three surfaces were given identical treatment and, hence, the relative values of the contact angles are a true representation of the actual differences in the contact angles. The results of the contact angle measurements are presented in Table 2. Four sets of measurements are presented here. It can be seen that gold has a much higher contact angle as compared to copper and nickel. It should be noted that dynamic contact angle is usually much higher than the static contact angle, therefore these measurements are not really representative of the actual situation. However, for the purpose of this study, it is sufficient to note the relative magnitudes of the contact angles.

Table 2 Contact angle

Material	Contact angle θ, deg
Copper	47 ± 3
Nickel	48 ± 4
Gold	63 ± 4

Table 3 Roughness

	Roughness	
Material	R_q, μm	R_p, μm
Copper	0.08	0.20
Nickel	0.08	0.20
Gold	0.11	0.20

Table 3 provides the roughness values R_q, R_p of the copper, nickel, and gold surfaces prepared with 14-μm emery paper. It is noted that the values of the surface roughnesses is comparable. Here, R_q is the geometric average roughness defined as the rms of the roughness heights about a mean line. R_p is the maximum height of the profile above the mean line within the assessment length.

Figure 7 shows the effect of the contact angle on heat transfer characteristics for a water flow rate of 4 liters/h and an air flow rate of 0.16 l/s. As can be seen, there is a definite increase in slope for gold at around 100°C as compared to copper, and thereafter the gold surface gives a higher heat flux until at around dryout where all the curves begin to merge. The nickel surface curve lies between gold and copper as would be expected. This leads us to believe that the higher contact angle of gold enhances nucleation further than for the copper or nickel surfaces.

Figures 8 and 9 show the effect of the surface material at a flow rate of 1 l/h and 2 l/h of water, respectively, and at an air flow rate of 0.16 l/s. Fourteen-micrometer emery paper was used for polishing. Again the trends are as those mentioned for the case of Fig. 7. It is observed that at the lower water flow rate the effect was less pronounced than for the higher water flow rate. Three mechanisms come into play in such a comparison.

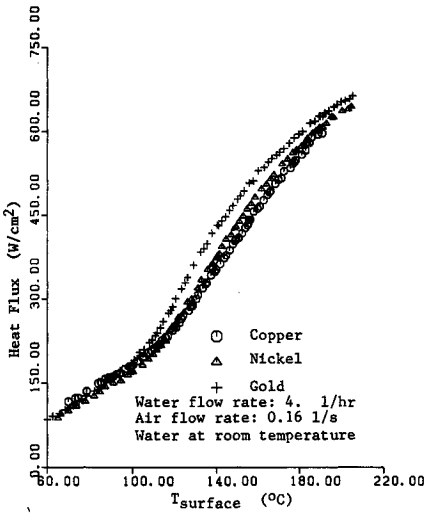

Fig. 7 Effect of surface material properties.

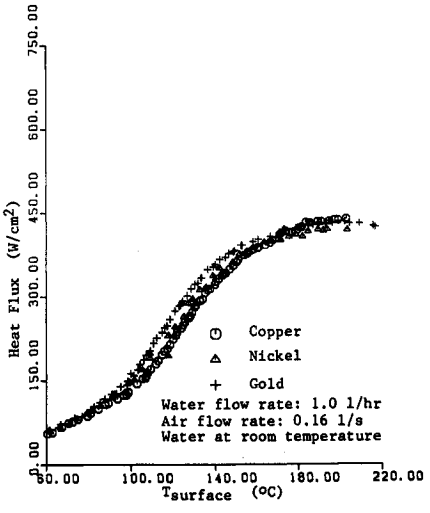

Fig. 8 Effect of surface material properties.

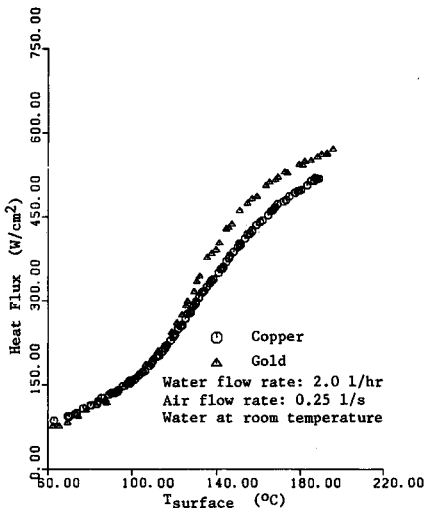

Fig. 9 Effect of surface material properties.

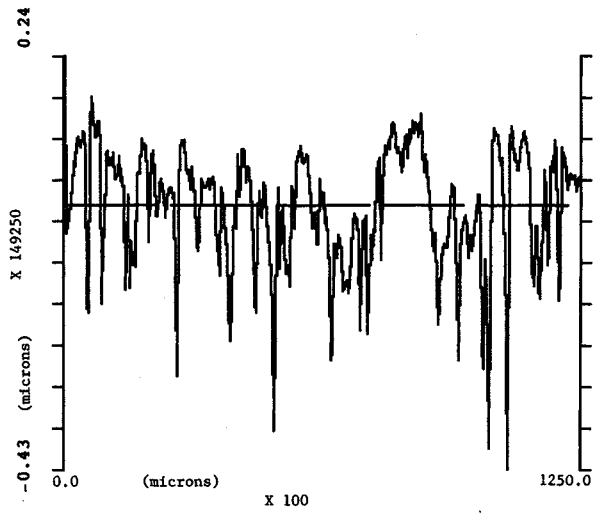

Fig. 10a Surface profile of the 14-μm grit polished surface.

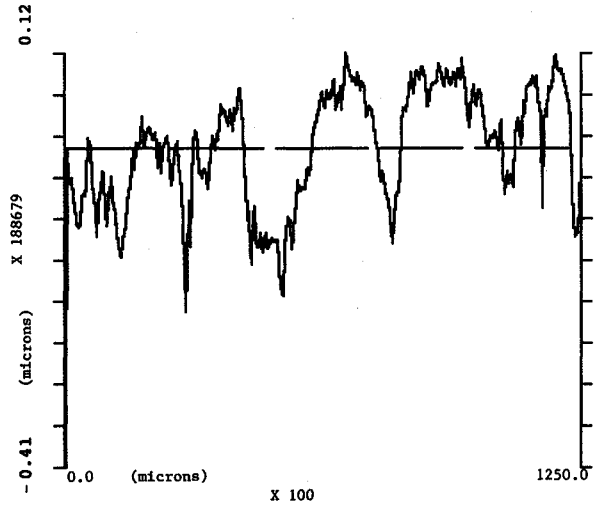

Fig. 10b Surface profile of the 0.3-μm grit polished surface.

1) The higher contact angle provides a better possibility for nucleation and, hence, enhanced heat removal.

2) The higher contact angle provides a more stable and surface adhering bubble. Because the nucleating bubbles are not swept away instantly by the faster flow and are able to reach some optimum size before ejection, thus providing a higher contribution to phase change heat transfer.

3) The high subcooling at the higher flow rates delays the onset of nucleation (100°C for 1 l/h and 110°C for 2 l/h). Increasing the air flow rate tends to thin out the film and increases the convection, thus initially nucleation is more or less suppressed at higher air flow rates. Experiments to study the effect of increased air flow rates (>0.25 l/s) for different surface materials, indicate that the heat transfer capability of all three surfaces are very close, though the gold surface still shows a little higher heat flux between 100°C and the saturation region. The saturation heat flux under such conditions is same for all the materials.

Surface Roughness Effects

Two different surface roughnesses were studied. These were the 14-μm grit polish and the 0.3-μm grit polish on a copper surface. The surface profiles for these two surfaces were measured (the surface profiles for the gold and nickel surfaces were also measured) using a diamond tip profilometer. The profiles are shown in Figs. 10a and 10b, respectively. The experiments were then performed on the smoother surface and the results compared with the results obtained earlier using the rougher surface.

As shown in Fig. 11, something startling happens at around 80°C for the smoother surface. The heat flux just shoots up at near constant temperature and later an increase in temperature shows an increase in heat flux (the surface temperature was not increased into the dryout regime for the fear of oxidizing this highly polished surface). As can be seen the increase is almost 40–50% in heat flux at any temperature above 80°C. This steep increase in heat flux is because a very smooth surface provides 1) a liquid film thin enough to evaporate, by conduction through the liquid film, from the free surface; and 2) a decrease in vapor pressure at the free surface caused by the air flowfield. This secondary flow of air causes the liquid to evaporate at a temperature much lower than its saturation temperature at atmospheric pressure. A detailed description of this effect is provided in Ref. 19.

This phenomenon of a steep rise in heat flux without change in surface temperature provides 1) a very efficient means of heat removal at a very low surface temperature; and 2) the heat dissipation can increase by a large amount without altering the surface temperature. This can be of great advantage in applications where varying heat fluxes have to be dissipated

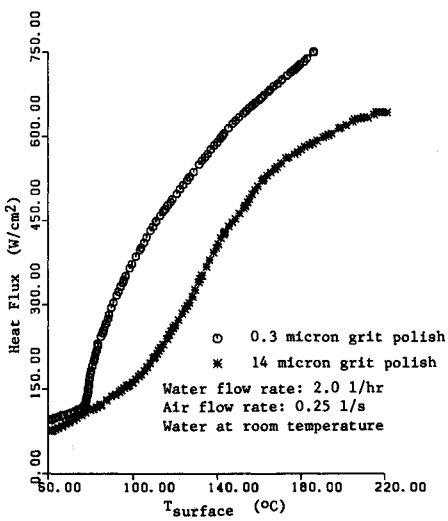

Fig. 11 Effect of roughness.

but, the temperature has to be maintained within narrow limits.

The effect of surface roughness for rougher surfaces (i.e., rougher than the 14-μm grit polished surface) was also studied. It was found that any surface rougher than the threshold of a 0.3-μm surface polish had no noticeable enhancing heat transfer effect.

Uncertainty Analysis

The heat flux is calculated by using Fourier's law of heat conduction across the constantan film to give

$$q = k_{Co} (\Delta T_{Co}/\Delta x_{Co}) \tag{6}$$

Here, q is a function of ΔT and Δx. Then the uncertainty (elemental propagation of errors being taken into account) in the value of q obtained using measurements of ΔT and Δx is given by

$$w_q = \pm \sqrt{\left(\frac{K}{\Delta x} w_T\right)^2 + \left(\frac{K\Delta T}{\Delta x^2} w_x\right)^2} \tag{7}$$

where w_T and w_x are the uncertainties in the measurement of the temperature across and the thickness of the constantan film and w_q is the uncertainty in the heat flux. When the uncertainty is represented as a ratio of

$$w_q' = 100\, w_q/q \tag{8}$$

and an uncertainty analysis performed using Eqs. (7) and (8) over the presented data it is observed that $w_q' \leq 10\%$. The uncertainty in the surface temperature is $w_{T\text{surf}} \leq 1.6\%$.

Conclusions

The ability of three different surfaces of copper, nickel, and gold to dissipate heat under conditions of spray cooling using air atomized nozzles was studied. Heat flux rates were obtained for two different rough surfaces for liquid flow rates of 1–4 l/h and air flow rates of 0.1–0.4 l/s.

In conclusion, the following points may be noted:

1) A higher water flow rate results in an increase in heat flux partially due to the increased convection resulting from the increased local heat transfer coefficients in the region of droplet impact.

2) A higher air flow rate results in an increase in heat flux due to a) an increase in air flow rate increases the momentum of water drops and thus increases local convection; b) increasing the air flow rate results in a decrease in the liquid film thickness, this enhances the evaporation from the free liquid surface; and c) removal of vapor evolving from the liquid film improves by increasing the air flow rate, this results in reduced partial pressure of water vapor near the free surface of the film, which in turn reduces the phase change temperature in that region. Air flow rate was shown to have greater effect as compared to water flow rate for moderate temperatures (100–160°C).

3) A higher coolant temperature gives a lower heat flux below the boiling point temperature, but later the heat flux vs temperature curve shows a higher slope than the cooler spray case. The maximum heat flux obtained is lower for the hotter spray because of the reduction in sensible heating of water.

4) A higher contact angle promotes nucleation and, hence, shows a higher heat flux between 100°C and CHF. This effect (though not as pronounced as that due to an increase in air or water flow rate), leads to the conclusion that nucleation does play a major role in spray cooling.

5) A very smooth surface (better than 0.3-μm polish) shows a dramatic increase in heat flux due to the thinner liquid film which causes the liquid to evaporate from the free surface through direct conduction.

This study has shown that nucleation does in fact influence the heat transfer process in spray cooling. Also, that a very smooth surface can dissipate a very high heat flux at low temperatures. The contribution of various heat transfer phenomena such as conduction, convection, and nucleation remains uncertain because of the very complex nature of the spray cooling process and the difficulty in measuring the liquid film thickness. Attempts are being made to measure the liquid film thickness. Numerical modeling and experimental work is also under way to determine the effect of parameters such as droplet size, velocity, and distribution in order to arrive at a means of predicting the heat transfer through correlations.

Acknowledgments

This work was supported by Wright Research and Development Center, Contract F33615-87-C-2777. Micheal Morgan was the technical monitor. The authors acknowledge the technical assistance of E. B. Yates and Joel Kern for the fabrication of the experimental components.

References

[1]Choi, K. J., and Yao, S. C., "Mechanism of Film Boiling Heat Transfer of Normally Impacting Spray," *International Journal of Heat and Mass Transfer*, Vol. 30, No. 2, 1987, pp. 311–318.

[2]Goldstein, M. E., Yang, W-J., and Clark, J. A., "Momentum and Heat Transfer in Laminar Flow of Gas with Liquid-Droplet Suspension Over a Circular Cylinder," *Journal of Heat Transfer*, Vol. 89, 1967, pp. 185–194.

[3]Pais, M. R., Tilton, D., Chow, L. C., and Mahefkey, E. T., "High Heat Flux Low Superheat Evaporative Spray Cooling," AIAA Twenty-Seventh Aerospace Sciences Meeting, Reno, NV, AIAA-Paper 89-0241, 1989.

[4]Cole, R., "Boiling Nucleation," *Advances in Heat Transfer*, Vol. 10, 1974, p. 85.

[5]Berenson, P. J., "Experiments on Pool Boiling Heat Transfer," *International Journal of Heat and Mass Transfer*, Vol. 5, 1962, pp. 985–999.

[6]Kurihara, H. M., and Myers, J. E., "The Effects of Superheat and Surface Roughness on Boiling Coefficients," *AIChE Journal*, Vol. 6, No. 1, 1960, pp. 83–91.

[7]Webb, R. L., "The Evolution of Enhanced Surfaces Geometries for Nucleate Boiling," *Heat Transfer Engineering*, Vol. 2, 1981, Nos. 3–4, pp. 46–69.

[8]Parizhskiy, O. V., "Study of Boiling Heat Transfer with a Failing Film of Refrigerant," *Heat Transfer—Soviet Research*, Vol. 4, No. 4, 1972, pp. 43–47.

[9]Kopchikov, I. A., et al., "Liquid Boiling in a Thin Film," *International Journal of Heat and Mass Transfer*, Vol. 12, 1969, pp. 791–796.

[10]Corty, C., and Foust, A. S., "Surface Variables in Nucleate Boiling," *AIChE, Chemical Engineering Progress Series*, Vol. 51, No. 17, 1955, pp. 1–12.

[11]Liaw, S. P., and Dhir, V. K., "Effect of Surface Wettability on Transition Boiling Heat Transfer from a Vertical Surface," *Eighth International Heat Transfer Conference*, San Francisco, Vol. 4, Hemisphere, Washington DC, 1986, pp. 2031–2036.

[12]Tong, W., Bar-Cohen, A., Simon, T. W., and You, S. M., "Contact Angle Effects on Boiling Incipience of Highly Wetting Liquids," *International Journal of Heat and Mass Transfer*, Vol. 33, No. 1, 1990, pp. 91–103.

[13]Maracy, M., and Winterton, R. H. S., "Hysteresis and Contact Angle Effects in Transition Pool Boiling of Water," *International Journal of Heat and Mass Transfer*, Vol. 31, No. 7, 1988, pp. 1443–1449.

[14]Defay, R., Prigogine, I., Bellemans, A., and Everett, D. H., *Surface Tension and Adsorption*, Wiley, New York, 1966, pp. 342–346.

[15]Bankoff, S. G., "Entrapment of Gas in the Spreading of a Liquid over a Rough Surface," *AIChE Journal*, Vol. 4, 1958, pp. 24–26.

[16]Jussin, E., *Stopping Time: The Photographs of Harold Edgerton*, Abrams, New York, 1988.

[17]Griffith, P., and Wallis, J. D., "The Role of Surface Conditions in Nucleate Boiling," *Chemical Engineering Progress Symposium Series*, Vol. 56, No. 30, 1960, pp. 49–63.

[18]Pais, M. R., and Singh, S. N., "A Fourier Analysis Approach for Surface Definition and the Effect of Roughness on the Local Convective Heat-Transfer Coefficient as Related to Ice Accretion," AIAA Twenty-Sixth Aerospace Sciences Meeting, Reno, NV, AIAA Paper 88-0117, 1988.

[19]Pais, M. R., Chow, L. C., and Mahefkey, E. T., "Surface Roughness and Its Effects on the Heat Transfer Mechanism in Spray Cooling," ASME Winter Annual Meeting, San Francisco, Heat-Transfer Div., Vol. 119, 1989, pp. 51–59.

[20]Dhir, V. K., and Tung, V. X., "A Thermal Model for Fully Developed Nucleate Boiling of Saturated Liquids," ASME Winter Annual Meeting, Chicago, IL, 1988.

[21]Mesler, R., "A Mechanism Supported by Extensive Experimental Evidence to Explain High Heat Fluxes Observed During Nucleate Boiling," *AIChE Journal*, Vol. 22, No. 2, 1976, pp. 246–252.

[22]Hospeti, N. B., and Mesler, R. B., "Vaporization at the Base of Bubbles of Different Shape During Nucleate Boiling of Water," *AIChE Journal*, Vol. 15, 1969, pp. 214–219.

[23]Berenson, P. J., "Transition Boiling Heat Transfer from a Horizontal Surface," MIT Heat Transfer Lab., TR 17, 1960.

[24]Faneuff, C. E., McLean, E. A., and Scherrer, V. E., "Some Aspects of Surface Boiling," *Journal of Applied Physics*, Vol. 29, No. 1, 1958, pp. 80–84.

[25]Hsu, Y. Y., "On the Size Range of Active Nucleation Cavities on a Heating Surface," *Journal of Heat Transfer*, 1962, pp. 207–216.

[26]*Marks' Standard Handbook for Mechanical Engineers*, 8th ed., McGraw Hill, New York, 1978, Chaps. 4, 13.

[27]Pais, M. R., Chow, L. C., and Mahefkey, E. T., "Rotating Jet Impingement Cooling," AIAA Twenty-Seventh Aerospace Sciences Meeting, Reno, NV, AIAA Paper 89-175, 1989.